

HWNet v2: An Efficient Word Image Representation for Handwritten Documents.

Praveen Krishnan · C.V. Jawahar

Received: date / Accepted: date

Abstract We present a framework for learning an efficient holistic representation for handwritten word images. The proposed method uses a deep convolutional neural network with traditional classification loss. The major strengths of our work lie in: (i) the efficient usage of synthetic data to pre-train a deep network, (ii) an adapted version of the ResNet-34 architecture with the region of interest pooling (referred to as HWNet v2) which learns discriminative features for variable sized word images, and (iii) a realistic augmentation of training data with multiple scales and distortions which mimics the natural process of handwriting. We further investigate the process of transfer learning to reduce the domain gap between synthetic and real domain, and also analyze the invariances learned at different layers of the network using visualization techniques proposed in the literature.

Our representation leads to a state-of-the-art word spotting performance on standard handwritten datasets and historical manuscripts in different languages with minimal representation size. On the challenging IAM dataset, our method is first to report an mAP of around 0.90 for word spotting with a representation size of just 32 dimensions. Furthermore, we also present results on printed document datasets in English and Indic scripts which validates the generic nature of the proposed framework for learning word image representation.

Keywords Word image representation, handwritten and historical documents, word spotting, convolutional neural networks.

1 Introduction

Digitization of documents has opened numerous possibilities in providing widespread access to information and creating data for building language processing pipelines such as machine translation and search engines. These digitized documents are either machine printed or handwritten and include books, manuscripts, letters, invoices, catalogs etc. Content-level access to this extensive digital corpus is possible only by learning an efficient representation of document images which is rich in preserving both lexical and semantic information. In this work, we set our granularity at the level of words, and focus on representing word images in a feature space which preserves its lexical information.

Content level access can be achieved either through “recognition” or “retrieval”. Given the advancements in the field of information retrieval and language processing, one can build robust and innovative solutions using the text produced from an ideal recognizer. However, the document images that we are interested in this work are handwritten, historical manuscripts and degraded printed books where traditional printed Optical Character Recognizer (OCR) based methods would result in noisy text and could lead to inferior results. This leads us to the complementary method, where the idea is to formulate the problem from a “retrieval” perspective in either recognition-based [17, 80] or recognition-free [4, 45, 67] manner. In this setting, given a query word image, one has to rank all the word images from

Praveen Krishnan
CVIT, IIIT Hyderabad, India
E-mail: praveen.krishnan@research.iiit.ac.in

C.V. Jawahar
CVIT, IIIT Hyderabad, India
E-mail: jawahar@iiit.ac.in

the candidate set in the order of its similarity. This idea was popularized as ‘word spotting’ in [45]. Here both the query and the candidate word images are represented using a holistic representation which captures the lexical information of a word in an appropriate feature space. The design of these holistic representations is one of the major challenges to be solved, which decides the effectiveness of recognition-free methods. In this work, we propose a new holistic descriptor for word images which can seamlessly be used for developing applications involving handwritten and printed documents. We assume the segmentation of document images into words is given to us either in the form of ground truth or made available using external word proposal method which could be noisy. The proposed representation in this work is a word-level descriptor.

Feature engineering has been a key investigation for any pattern recognition problem. In the domain of document images, the problem of defining an optimal feature which describes a word [2, 4, 45, 68], character/patch [58, 65, 79] has been an interesting quest in the community over the last two decades. With the improved representations over time, there has been a significant impact on the larger goals of the community such as recognition and retrieval of documents, script recognition, layout analysis, etc. In the domain of word images, initial features proposed were based on pixel level statistics [46, 54] which worked only on limited settings of the writers and font variations. Later, with the popularization of local gradient level features in computer vision such as scale-invariant feature transform (SIFT) [41] and histogram of gradients (HOG) [12], are adapted to document images due to their generic properties. These features are invariant to scale, translation, and common degradation. The bag of visual words (BOW) [11, 73], were built using these local features along with advanced encoding schemes such as Fisher [50], locality constrained linear coding (LLC) [82], and sparse codes [87]. These features along with the learned models such as [4], obtained state-of-the-art word spotting and recognition for historical manuscripts and multi-writer handwritten documents.

More recently, there has been a paradigm shift from ‘feature engineering’ to ‘feature learning’ due to the resurgence of neural networks. It is mostly credited to the revival of convolutional neural networks (CNN) [39], availability of large scale of annotated data [14], and increased computing power using graphical processing units (GPU). The features are learned on the fly during training and gets adapted to the task of interest. Networks trained on large data sets also learn generic feature representation that can be used



Fig. 1: Sample top-1 nearest neighbors in the learned representation space. Here we show examples from historical datasets which contains degradation and irregular segmentation of words. One can also notice invariance of representation in terms of handwriting variations as shown in the top row.

for related tasks [56], and in many cases, have reported state-of-the-art results as compared to the handcrafted features. When the data is limited, fine-tuning a pre-trained network has also been demonstrated to be very effective. In the domain of document images these features have shown better performance for word spotting [37, 74, 76, 83], recognition [52], document classification [26], layout analysis [10], etc. In this work, we propose a deep CNN architecture named as HWNet v2, for the task of learning an efficient word level representation for handwritten documents which can handle multiple writers and, is robust to common forms of degradation and noise. We also show the generic nature of the proposed representation and architecture which allows it to be used as an off-the-shelf feature for printed documents and in building state-of-the-art word spotting systems for various languages. In order to derive a compact representation for an efficient storage and retrieval, we evaluate the performance of compressed feature codes, where we push the compression to an order of 16-to-32 dimensions with minimal drop in performance. Fig. 1 shows sample word images which are considered as nearest neighbors in the proposed representation space. The shown images are quite challenging in terms of handwriting variations, distortion created due to scanning, and irregular segmentation which are common in historical manuscripts. These images are taken from the test sets of the datasets used in this work, which are explained more in detail in Section 7.

1.1 Contributions

The baseline CNN architecture HWNet considered in this work was first proposed in [37], which first demon-

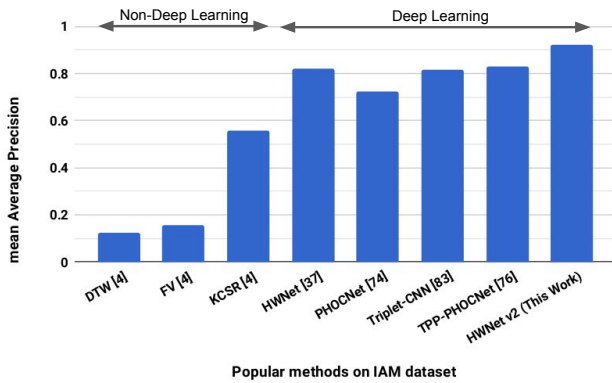


Fig. 2: Evolution of word spotting methods from the perspective of different word image representation schemes. The evaluation is conducted on the IAM [47] dataset using mean Average Precision (mAP). More details on evaluation scheme and dataset is provided in Section 7.1.

strated the use of such an architecture in learning an efficient word level representation. This work is dedicated entirely to enrich the representation space and learning better in-variances that are common to the handwritten data. The major contributions of this work are: (i) bringing architectural improvements by making it more deep with the help of residual connections, referred as HWNet v2, (ii) use of multi-scale training and region of interest pooling (ROI) to support variable sized word images, (iii) use of extensive augmentation scheme with elastic distortion which is better suited for handwritten images. In addition to this, we perform an in-depth analysis of transfer learning at various layers and also visualize the features at different layers of the network to get better insights on the learned features and its invariances. We also significantly compress our representations for efficient storage and faster retrieval. We further extend our experiments on newer datasets from historical documents and degraded printed books from Indic scripts and present state-of-the-art results on standard datasets.

2 Related Works

There are numerous successful attempts done in the past which focus on different aspects of the problem such as the modality of data (printed, handwritten and scene text), nature of representation either fixed or variable length, and type of embedding scheme. We broadly split our discussion on related works into three major parts: (i) the classical methods built using variable length representation schemes, (ii) fixed length representation which are achieved using bag of words frame-

work, and (iii) learned representation using, different classifier models built on top of handcrafted features and using the deep learning networks. Fig 2 presents an evolution of some of the key methods proposed in the space of word spotting, which uses some of the recent representations proposed for handwritten word images. As one can notice, with the introduction of deep learning, there has been a significant boost in the performance. Our proposed method, which is shown in the end further boosts the performance in this space. In Table 1, we present a quick overview of the related works that we discuss in this section based on its representation type. One can also refer to the detailed survey presented in [21] which reviews major representation schemes proposed for the task of word spotting.

2.1 Classical Representation

Learning holistic representation for word images was popularized as word spotting which was originally proposed in [60] for speech processing. Within the document community, initial attempts in this space mostly focused on variable length representations of word images by considering it as a temporal sequence. Most of these methods used profile features [45, 46, 54] which are computed at each column of the word image and are summarized using various pixel level statistics. Dynamic Time Warping (DTW) based algorithms were found to be useful for matching variable length representations and is quite popular in speech [49, 69] and other sequence matching problems. In [54], Rath et al. used profile features namely vertical profile, upper & lower word profile, and background to ink transitions. In [7, 48], profile features were combined with the shape based structural features for a partial matching scheme using DTW. Although these features

Table 1: Overview of major methods proposed in the literature, summarizing different types of word image representation schemes.

Method	Representation
Profile [54] Profile+Moments [46] Profile+DFT [40] Slit HoG [79]	Variable Length
Local Gradient Histogram [58] SIFT [63]	HMM
SIFT [1, 2, 67, 70, 86]	BoWs
SIFT [3]	Fisher
SIFT [4]	PHOC Attributes
Deep Learning [37]	Neural Codes
Deep Learning [35, 74, 75, 83]	PHOC Attributes
Deep Learning [24]	Levenshtein Embedding

are fast to compute, it is susceptible to noise and common degradation present in documents.

With the popularity of the local gradient features such as SIFT [41], HOG [12] which describes a patch using histograms of edge orientations computed from a gradient image, the features are less susceptible to stray pixels and variations in brightness and contrast. Methods such as [58, 79] adapted local gradient features for word spotting where [79] used a continuous DTW algorithm for partial word matching from the line images and [58] used Hidden Markov Model (HMM) based classification method. Most of the features discussed above are not robust to different fonts, writing styles and required careful image pre-processing techniques such as binarization, slant and skew correction which remain hard for handwritten and historical documents. Moreover, the methods such as DTW and HMM based scheme of matching variable length representations do not scale to large datasets due to the higher time complexity. Hence, the later methods appreciated more on fixed length representations built on top of highly engineered features proposed in computer vision.

2.2 Bag of Word Representation

The popularity of bag of words (BOW) [11, 73] framework using local gradient features such as SIFT and HOG, led to its proliferation to document images [1, 2, 67, 68, 70, 86]. Rusinol et al. [67, 68], presented a patch based framework using BOW histograms computed from the underlying SIFT descriptors. The histogram based representation was further projected onto a topic space using latent semantic indexing (LSI) [13], where the latent topic space is assumed to preserve the lexical content of word images. In [70, 86], BOW based representation was adapted for word image retrieval for machine printed documents using standard keypoint detectors such as Harris [27], FAST [62] corner detectors, while the local features at the keypoints were computed using SIFT. Due to the fixed length and sparse nature of the representation, the matching was done using cosine distance and an inverted index was used for faster retrieval. Aldavert [2] et al., presents a detailed survey for BOW based representation for handwritten word spotting with its analysis on the effect of codebook size, choice of encoding, and type of normalization. In a similar line of work using local features and codebook, Almazán et al. [3] uses an exemplar-SVM [44] for representing a query and performs the initial scoring of candidate words. Given the initial matches, the list is re-ranked using a Fisher vector based representation [51] which is a generalization of BOW using higher order statistics. In general, the unsupervised nature of learning of BOW

based methods make them directly applicable to historical databases where the annotation is hard and costly. However, the limitation of local features (SIFT, HOG) to capture the larger part level information from word images restricted these methods to work only for limited writer datasets where the variations are less.

2.3 Learned Representations

Learning representation in supervised settings leads to better discriminative features at the cost of annotations. Here, we present popular methods from literature which uses label embedding techniques together with traditional machine learning models and modern deep learning architectures.

2.3.1 Word Attributes

Almazán et al. [4] proposed a label embedding approach where both word images and the corresponding labels are embedded into a common vectorial subspace which allows comparing both modalities seamlessly. The method uses a new textual representation referred to as pyramidal histogram of characters (PHOC), which concatenates the histogram of characters at multiple spatial regions in a pyramidal fashion. Here, each feature denotes the presence or absence of a particular character at a particular spatial region and is called a character level attribute. Similar to the textual representation, PHOC representation for word images could be derived from the scores of attribute level binary classifiers, which are learned from training word images which possess that particular attribute. In [4], Almazán et al. uses Fisher features of word images for learning word image attributes while PHOC for text labels are extracted by the spatial position of each character. Although the word attribute framework is generic, the underlying handcrafted features limit the robustness of the learned holistic features. In recent methods, this is addressed using deep neural networks to learn features in an end to end hierarchical manner which results in better generalization.

2.3.2 Deep Learning

With the advancements in deep learning, there is a paradigm shift in feature engineering where features are now learned during the training process which customizes itself to the domain of training data. Among different types of neural networks, deep convolutional neural networks (CNN) [39, 72, 77] have revolutionized the way features are learned for specific tasks. In the domain of word images, Jaderberg et al. [31–33], proposed

three different architecture models (char, nGram and dictionary words) for scene text recognition. Taking inspirations for word attributes, for handwritten images, Poznanski et al. [52] adapted VGGNet [72] for recognizing PHOC attributes by having multiple parallel fully connected layers, each one predicting PHOC attributes at a particular level. In similar spirits, different architectures [35, 74, 76, 83] were proposed using CNN networks which embed features into different textual embedding spaces defined by PHOC. In [74], Sudholt et al. proposes an architecture to directly embed image features to PHOC attributes by having sigmoid activation in the final layer and thereby avoiding multiple fully connected layers as presented in [52]. It is referred to as PHOCNet, which uses the final layer activation to derive a holistic representation for word spotting. In the later set of works [75, 76] from the same group, PHOCNet was adapted with temporal pooling layer (TPP-PHOCNet) and evaluated under different loss functions and optimization algorithms which further improved the word spotting performance. In [35, 36], the features computed from HWNet [37] are embedded into word attribute space by training attribute based SVM classifiers and projecting both image and textual attributes to a common subspace. In [83], the authors propose a two stage architecture where a triplet CNN network is trained to reduce the distance between the anchor word image and a similar labeled (positive) word image, while simultaneously increasing the distance between the anchor and negative labeled word image. In the second stage, the learned image representation is embedded into a word embedding space (PHOC, DCTOW, ngram etc) using a fully connected neural network. In the above methods where the target embedding is an attribute space, one can query the representation space either using query-by-string or query-by-example setting.

In general, most of these methods learn representation restricted to a fixed attribute space whereas, in this work, our aim is to learn a generic representation for word images derived by formulating a proxy task of word image classification. We derive our representation from the penultimate layer before the softmax which takes the advantage of the hierarchical composition of concepts in a deep network where higher layers tend to capture parts and attribute level information. In terms of architecture advancements, we use a much deeper network using residual connections and present variable sized images without distorting the aspect ratio of word images. The learned representation can be used for word attribute learning [35, 36], spotting, and retrieval tasks for both handwritten and printed documents irrespective of the vocabulary used while training.

2.4 Segmentation-Free Approaches

In addition to the different representation schemes, one can also classify the methods in terms of segmentation-based and segmentation-free word spotting approach. Most of the methods presented so far belong to the setting where the segmentation of words is available in the form of ground truth. In segmentation-free setting, the input is a page image and the underlying method first proposes potential word hypothesis before computing its representation. In literature, one can place the segmentation-free approaches into three broad categories. The first category of methods [3, 20, 63, 67] use a sliding window technique where the regions are proposed along a regular grid. This typically results in a dense extraction of bounding boxes and are computationally expensive to process. The second category of methods utilize connected components [19, 34] along with mathematical morphological operations to extract characters/words from the page image. Most of these methods work in a bottom-up fashion and utilize certain rules to extract the final bounding box of words. The number of proposals obtained using this approach is far less than sliding windows, however, they are sensitive to page quality and degradation as seen in historical documents. In [64], authors propose a hybrid approach where the document image is first subjected to dense text detection using sliding windows and later the word hypotheses are computed using the set of extremal regions. The third category of methods [6, 84, 85] in the segmentation-free setting is inspired by the recent success of region proposal based object detection techniques such as Faster R-CNN [57]. The Ctrl-F-Net [84] model proposes an end to end trainable detection and embedding network. It utilizes a localization layer to predict potential word proposals along with its wordness score. The initial predictions are further filtered and presented to the embedding network. The method also utilizes a complementary external region proposal method called as Dilated Text Proposals (DTP) to improve the overall recall of the system. The authors extended their method in [85] by simplifying the architecture (Ctrl-F-Mini) by only utilizing the external proposals computed using DTP. This performs faster and better in certain situations than the original architecture.

3 Handwritten Synthetic Dataset

Quality data [14, 16] has always played a pivotal role in the advancement of pattern recognition problems. Some of the key properties for any dataset are: (i) a good sample distribution which mimics the real world

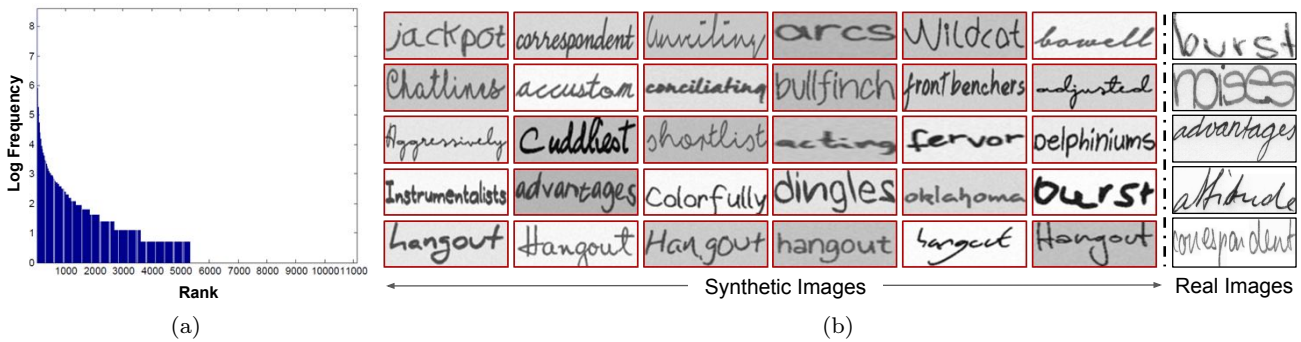


Fig. 3: (a) Distribution of words in IAM dataset, (b) Sample word images from the IIIT-HWS dataset created as part of this work, to address the lack of training data for learning deep CNN networks.

unseen examples, (ii) quality of annotation, and (iii) scale. With the success of deep learning based methods [32, 39, 72, 77], there has been a surge in newer supervised learning architectures which are ever more data hungry. These architectures have millions of parameters to learn, thereby need a large amount of training data to avoid over-fitting and to generalize well. In general, data creation is a time consuming and expensive process which requires huge human efforts. More recently, an alternative form of data generation process with minimal supervision is getting popular [32, 61, 66], which uses synthetic mechanisms to render and annotate images in an appropriate form. The simple idea of generating data synthetically allows overcoming the challenges in obtaining the data. In this work, we address the need for large scale annotated datasets for handwritten images by generating synthetic words with natural variations. Fig. 3 (b) shows sample handwritten word images generated using the proposed framework which looks quite natural and comparable with its counterparts from the real world which are shown in the last column of the figure.

Some of the popular datasets in handwritten domain are IAM handwriting dataset [47], George Washington [18, 45], Bentham manuscripts [9], Parzival database [18] etc. Except for IAM, the remaining datasets are part of the historical collections which were created by one or very few writers. IAM is a relatively modern dataset, which consists of unconstrained text written in forms by around 657 writers. The vocabulary of IAM is limited to nearly 11K words whereas any normal dictionary in the English language would contain more than 100K words. Fig. 3 (a) shows the distribution of entire words in IAM vocabulary which follows the typical Zipf law. As one can notice that, out of 11K words, nearly 10.5K word classes contain fewer than 20 samples or instances. Also, the majority of remaining words are stop words which are

shorter in length and are less informative. The actual samples in training data are much smaller than this, which limits building efficient deep learning networks such as [39].

3.1 Handwritten Font Rendering

We use publicly available handwritten fonts for our task. The vocabulary of words is chosen from a dictionary. For each word in the vocabulary, we randomly sample a font and render¹ its corresponding image. During this process, we vary the following parameters: (i) kerning level (inter character space), (ii) stroke width, from a defined distribution. In order to make the pixel distribution of both foreground (F_g) and background (B_g) pixels more natural, we sample the corresponding pixels, for both regions from a Gaussian distribution where the parameters such as mean and standard deviation are learned from the F_g and B_g region of IAM dataset. Finally, Gaussian filtering is done to smooth the rendered image.

3.2 IIIT-HWS Dataset

To address the lack of data for training handwritten word images for English, we build a synthetic handwritten dataset of 1 million word images. We call this dataset as IIIT-HWS. Some of the sample images from this dataset are shown in Fig. 3 (b). Note that these images are very similar to natural handwriting. The IIIT-HWS dataset is formed out of 750 publicly available handwritten fonts. We use the popular Hunspell dictionary and pick a unique set of 90K words for this purpose. For each word, we randomly sample 100 fonts and render its corresponding image. Moreover, we prefer to

¹ We use ImageMagick for rendering the word images. URL: <http://www.imagemagick.org/script/index.php>

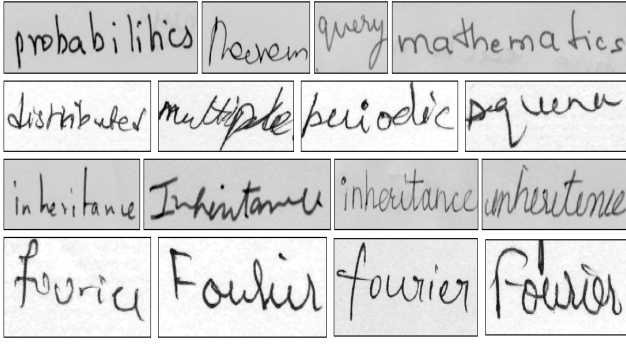


Fig. 4: Top two rows show the variations in handwritten images, the bottom two rows demonstrate the challenges of intra class variability in images across writers.

learn a case-insensitive model for each word category, hence we perform three types of rendering, namely, all letters capitalized, all letters lower, and only the first letter in caps.

4 HWNet

In the quest for learning better holistic features for word images, we leveraged recent CNN architectures to learn discriminative representations. Fig. 4 demonstrates the challenges across writers. The top two rows show the variations across images in which some are even hard for humans to read without enough context of nearby characters. The bottom two rows show different instances of the same word written by the different writers, e.g., “inheritance” and “Fourier”, where one can clearly notice the variability in shape for each character in the word image. The learned representation needs to be invariant to (i) both inter and intra class variability across the writers, (ii) presence of skew, (iii) quality of ink, and (iv) quality and resolution of the scanned image. One can also notice that there can be instances where few characters are completely distorted or degraded due to the cursive nature of word formation. However, the knowledge of vocabulary and its overall appearance, humans can still make out the word. One of the key differentiation of word images with respect to natural scene images is that a word image is inherently a variable length representation and making it fixed size would distort the individual characters non-uniformly.

We propose a deep CNN architecture named as HWNet, first presented in [37] for learning representation for handwritten word images, and further enhance the network capacity to address issues specific to handwriting. The improved network architecture is one of the major contributions of this work which is named as HWNet v2. We formulate the problem

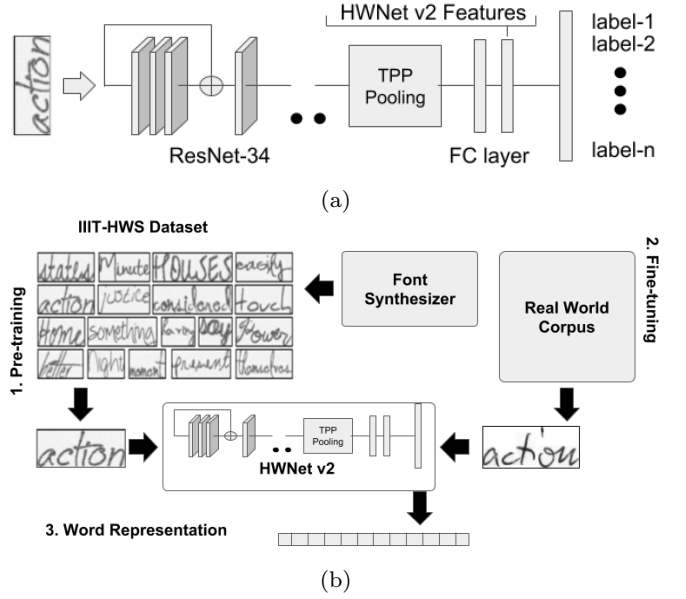


Fig. 5: (a) HWNet v2 architecture which comprises of a deep CNN architecture using ResNet blocks along with a TPP pooling and fully connected layers, (b) Flowchart showing the transfer learning process where we first pre-train the network on synthetic data and later fine-tune it on real corpus. The features are extracted from the penultimate layer of the network.

as word classification on a given vocabulary, however, given a trained network, we are interested to derive holistic features $f \in \mathbb{R}^d$ which obeys lexical similarity to all possible words in that language (irrespective of the trained vocabulary).

4.1 HWNet Baseline Architecture

In the baseline model, we use a fixed sized gray scale word image of dimension 48×128 . As noted earlier, this would result in distortion of aspect ratio, however, we show in experiments, the learned features are robust, and quite better than previous variable size representations. The underlying architecture of our CNN model is inspired from [39]. We use a CNN with five convolutional layers with 64, 128, 256, 512, and 512 square filters with dimensions: 5, 5, 3, 3 and 3 respectively. The next two layers are fully connected ones with 2048 neurons each. The last layer uses a fully connected (FC) layer with dimension equal to the number of classes (vocabulary of training and validation set), and is further connected to the softmax layer to compute the class specific probabilities. Rectified linear units (ReLU) are used as the non-linear activation units after each weight layer except the last one, and 2×2 max pooling is applied after

Table 2: Summary of the HWNet v2 network configuration. The width, height, and number of channels of each convolution layer are shown in square brackets, with the number of layers that are stacked together. We present two variations in the network (as shown in the sixth column), using a single level ROI pooling or using temporal pyramid pooling (TPP) with three levels.

Conv1	Block1	Block2	Block3	Block4	ROI/TPP	FC
3x3	[3x3,64] x 3	[3x3,128] x 4	[3x3,256] x 6	[3x3,512] x 3	ROI{6x12} TPP{1,2,3}	[2048] x 2

first, second, and fourth convolutional layers. We use a stride of one and padding is done to preserve the spatial dimensionality. We empirically observed that using batch normalization [30] after each convolutional and fully connected layer, resulted in lower generalization error as compared to dropouts. We use cross entropy loss function to predict the word class labels, and the weights are updated using the mini batch gradient descent algorithm with momentum.

5 HWNet v2

In our original HWNet architecture, we limited the number of convolutional layers to five, which was equivalent to layers proposed in AlexNet. More recently, newer architectures such as VGGNet [72], GoogLeNet [77], and ResNets [29] have shown deeper CNN networks for better performance and the resulting features to be more discriminative. Some of the key architectural changes brought in these networks, which lead to efficient training are: (i) use of lower dimensional filters (3×3) thereby having less parameters from larger sized filters, which also acts as a forced regularizer, (ii) use of (1×1) filters which acts as dimensionality reduction unit to keep the no. of parameters in control, (iii) use of inception layer [77] which introduces multi-scale processing by having multiple parallel layers operating at different scales, and (iv) use of residual blocks [29] to learn residual function $\mathcal{F}(x) := \mathcal{H}(x) - x$. Here $\mathcal{H}(x)$ is the desired underlying mapping. A residual layer is typically implemented using a shortcut connection without any parameters. In our improved HWNet architecture, named as HWNet v2, we use the ResNet34 [29] network with four blocks where each block contains multiple ResNet modules. Instead of using global average pooling (as proposed along with ResNet architecture [29]), we found fully connected layers in the end for learning better features from the penultimate layer. Table 2 shows the summary of HWNet v2 network configuration. Here each ResNet module consists of two convolutional layers

and a shortcut connection to enable residual learning. There is no max pooling in the network and the spatial resolution is down sampled using a stride of 2 at the first convolutional layer of block 2, 3 and 4. As stated earlier, we also use batch normalization after each convolutional and fully connected layer except the last one.

5.1 Multi-Scale Training and ROI/TPP Pooling

One of the major limitations in the previous architecture was the requirement to use fixed dimensional inputs so that it remains compatible with fully connected layers of the network. However as mentioned earlier, this leads to distortion of aspect ratio which manipulates the appearance of characters present in the word images arbitrarily. Another aspect which we tend to ignore so far due to the restriction of fixed size is, the ability to train word images in multiple scales so that the network remains invariant to multiple character scales. It has been observed that different writers typically write at different scales which leads to the presence of a variable sized sequence of characters. To overcome these issues, we use a fixed size padded image (128×384) to accommodate variable sized input word image. As shown in Fig. 6(a-b), we render different scale input image to learn scale invariant representation. Given the output feature maps from the last convolutional layer, we only keep the activations coming from the input region belonging to word image using ROI pooling. ROI pooling [22], layer gives a differentiable pooling (max/average) mechanism from vari-

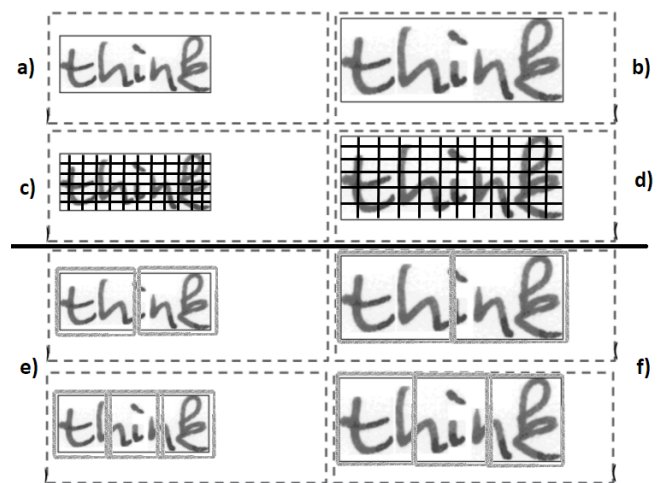


Fig. 6: (a-b) Multi-scale input, (c-d) region of interest pooling and, (e-f) temporal pyramid pooling shown at levels 2 and 3.



Fig. 7: Data augmentation techniques: affine and elastic distortion.

able sized input feature maps into fixed sized output maps, by constructing a grid with variable sized cells. Fig. 6(c-d), shows the ROI pooling where the number of grids in both images remains same while the size of each grid cell varies as per the scale of the image. In another variant of the HWNet v2 network, we use temporal pyramid pooling (TPP) similar to [75]. Both ROI and TPP takes variable length representation and produces a fixed length output depending on the number of grids. In our usage of TPP along HWNet v2, we follow a similar paradigm of creating pyramid levels only vertically [70, 75] with levels set at 1, 2 and 3. This would essentially capture the temporal properties present in the word image. Fig. 6(e-f), shows the temporal pyramid pooling at level 2 and 3. We also set max pooling as the preferred pooling operation within each grid for both ROI and TPP variants. In general, both ROI, TPP pooling methods don't require a fixed sized padded image. We made such a decision from an implementation point of view so that we can train in batches of images with the fixed size which wouldn't be possible otherwise.

5.2 Data Augmentation and Elastic Distortion

While training a CNN network, data augmentation [39] is a common practice to introduce artificial variations in data to make network robust to intra-class variations and prevent over-fitting. Popular data augmentation techniques are random crops, horizontal reflection, random flipping of pixels, and affine transformations such as scaling and translation. In this work, while training HWNet v2, we perform two major augmentation schemes which are: (i) affine transformation and (ii) elastic distortion. In affine transformation, we generalize to translation, scaling, rotation, and shearing. Here rotation and shearing are restricted to certain angles which mimic the skew and cursiveness present in natural handwriting. Elastic distortion [71] has been used in the past successfully for recognizing handwritten dig-

its. It mimics variations created from the oscillation of hand and inertia exerted on the writing medium. The basic idea is to generate a random displacement field which dictates the computation of new location to each pixel through interpolation. The displacement field is smoothed using a Gaussian filter of standard deviation σ and scaled using constant factor α . Both σ, α are set empirically by visualizing the quality of distorted images. Fig. 7 shows different possible variations created for each word image.

5.3 Curriculum Learning

Training with a large number of classes (10K for both HWNet and HWNet v2) typically results in slow convergence. To avoid such scenarios, we use the strategy from curriculum learning [8], where we start the training process from synthetic images showing easy examples (based on the number of characters) first and harder later. We also perform an incremental learning scheme where at initial epochs, we limit the number of classes to 500 and gradually increase the classes after achieving partial convergence. While increasing the number of classes, we copy the weights from last trained network and randomly initialize the newer weights. This improves the training process in terms of faster convergence in the presence of huge data (#classes).

5.4 Transfer learning

It is well-known that off-the-shelf CNNs [15, 56] trained for a related task could be adapted or fine-tuned to obtain reasonable and even state-of-the-art performance for new tasks. In our case, we prefer to perform transfer learning from the synthetic domain (IIIT-HWS) to real world setting. In general, real world handwritten labeled corpora are not large enough to train such deep networks which contain millions of parameters and can easily over-fit on smaller datasets. Moreover, the use of synthetic corpora would give us better vocabulary coverage and also capture some frequent patterns in ngrams which commonly occur in a particular language. In our case, transfer learning achieves to reduce the domain gap between the synthetic and real world data. We employ a similar approach as presented in [88], to do a careful study in transferring feature at a particular layer. The details of the study are presented in the experimental Section 7.5.

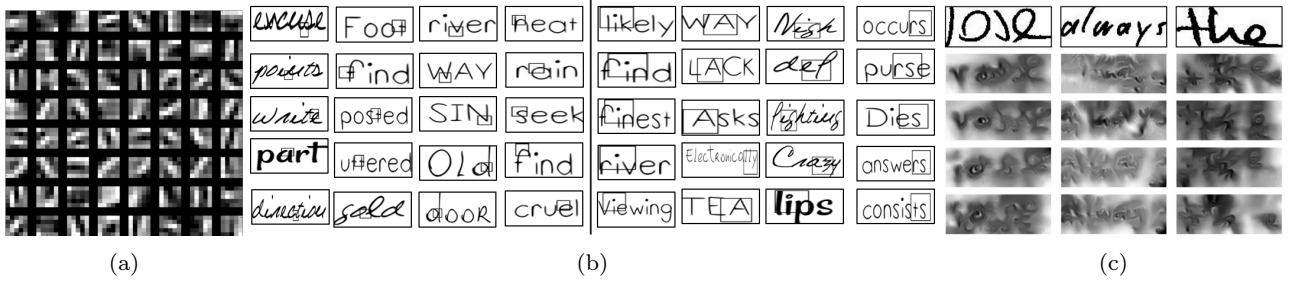


Fig. 8: Visualizations: (a) Layer 1 weights, (b) Visualization of the strongest activation [23] region of a particular neuron (each column refers to one neuron) of an intermediate convolutional layer. These regions are highlighted using a bounding box inside the word image. Here we notice that, in most of the cases, each neuron focus on detecting a semantically meaningful unit, and (c) Four possible reconstructions [43] of sample word images shown in columns. These are reconstructed from the representation obtained from the penultimate layer.

6 Visualizations

One of the most intriguing question while using a deep network is “what is the designated behavior of a neuron trained at a particular layer?”. The question is more relevant since we are dealing with a large scale training machine with millions of parameters. Some of the recent works [23, 43, 78, 89, 90] partly answer this question with meaningful insights on what happens behind the scenes.

Fig. 8 shows the visualization of the trained HWNet v2 architecture. It is easy to visualize weights for layer 1 since the filter dimension is $64 \times 1 \times 3 \times 3$ where we have: 64 output channels (#filters), 1 is the channel size since the input image is gray scale, and the spatial dimension of the filter is 3×3 . Fig. 8 (a) visualizes these weights which bear a resemblance to the Gabor filters and detects edges in different orientations. Visualizing neurons after layer 1 is non-trivial since the receptive field of these neurons keeps exploding and the filters are present in higher dimensions. Here we interpret these neurons using the non-parametric technique proposed in [23], which probes from the maximum neuron activations and visualizes the receptive fields in the original image. Fig. 8 (b) shows such interesting patches which correspond to the maximal activation of a particular neuron taken from a convolutional layer. Here, each column corresponds to one neuron activation for different word images and sorted in a descending order as per its activation values. The first four columns of the Fig 8 (b) correspond to a four arbitrary neurons/channels taken from ResNet block 1, Conv. 2 (ref. Table 2 for block details) where the size of effective receptive field is 15×15 pixels. The next four columns correspond to another set of four arbitrary neurons from ResNet block 2, Conv. 2 where the size of the receptive field is 37×37 . The maximal activation patch is highlighted in a black box. As one can notice, each column corresponds to a se-

mantically meaningful unit such as: Col1 neuron picks an inverted ‘v’ sort of unit, Col3 takes wedge behavior with patches coming from letters such as ‘v, W, N’ etc. while Col4 probes for a curve in the lower right quadrant. There also exists activation such as Row5, Col2 which does not make immediate sense in the original pixel space. The next set of columns (Col5-8) from the higher layer with more receptive field captures larger semantics such as: Col5 probes for the letter ‘i’ and a vertical line to its right, Col6 starts detecting capital letter ‘A’ and Col7-8 focuses partly on bigram level of information. Although we tried visualizing further layer, we couldn’t make much meaningful information since, the receptive field quickly explodes to larger regions which we believe could only be explored using techniques such as [89, 90].

Finally, we also interpret the features which are extracted from the penultimate fully connected layer using the optimization technique proposed in [43]. The basic idea is to invert the CNN features back to image space and arrive at possible images which have a high degree of probability for that encoding. This gives a better intuition of the learned layers and helps in understanding the invariances of the network. Fig. 8 (c) shows the possible reconstructions from three different representations. Here, we show the query images on the first row and its reconstruction in the following rows. One can observe that in almost all reconstructions, there are multiple translated copies of the characters present in the word image along with some degree of orientations. Similarly, we can see the network is invariant to the first letter being in a capital case (see Label: “the” at Row4, Col3) which was part of the training process. The reconstruction of the first image (see Label: “rose” at Row1, Col1) shows that possible reconstruction images include Label: “rose” (Row2, Col1) and “jose” (Row3, Col1) since there is an ambiguity in the query image.

7 Experiments

In this section, we empirically evaluate the proposed word image representation, perform ablation studies to understand the importance of each architectural component in HWNet v2 and explore the usefulness of the features for the printed domain in low resource languages such as Indic scripts. To evaluate the robustness of the feature, we take the task of word spotting, where given a query image we retrieve all similar word images from a given retrieval set.

7.1 Datasets

We use the four popular datasets in handwritten document analysis community out of which three are in English and one in German. Table 3 shows different datasets and their statistics in terms of the number of words and the number of writers in case of handwritten documents.

The IAM Handwriting Database [47]: It includes contributions from 657 writers making a total of 1,539 handwritten pages comprising of 115,320 words and is categorized as part of modern collection. The database is labeled at the sentence, line, and word levels. We use the official partition for writer independent text line recognition that splits the pages into training, validation, and test sets which are writer independent.

George Washington (GW) [55]: It contains 20 pages of letters written by George Washington and his associates in 1755 and thereby categorized into historical collection. The images are annotated at word level and contain approximately 5,000 words. Since there is no official partition, we use a random set (similar to [4]) of 75% for training and validation and the remaining 25% for testing.

Botany and Konzilsprotokolle [53]: These two datasets are parts of ICFHR 2016 Handwritten Keyword Spotting Competition [53]. The original competition contains data both segmentation based

and free scenario. We took only the segmentation based data which contained cropped word images split into training and test sets. There were also three partitions of training sets small, medium, and large. Here we took the largest partition for conducting experiments.

7.2 Evaluation Protocol

For comparing results across different methods under word spotting, we use the standard information retrieval evaluation measure, mean Average Precision (mAP), which is equal to the mean area under the precision-recall curve. The selection of queries follows the protocol used in [4], where we filter the stopwords from the test corpus while all words (including stopwords as distractors) are kept in the retrieval dataset in which the search is performed. Our major focus is on evaluating the features in the query by example setting (QBE). In this setting, since the query image is taken from the corpus, the first retrieved image is not included in the mAP calculation. Since Botany and Konzilsprotokolle datasets were part of keyword spotting competition where the query and retrieval set were given independently, the dropping of query image from retrieval set was not applicable. Also, note that all evaluations for English language datasets were done in a case-insensitive manner as followed by other related works.

7.3 Ablation Studies

Table 4 presents the ablation study to understand the key architectural changes and the role of data in improving the performance from HWNet baseline. These experiments are evaluated under word spotting for IAM dataset in the query by example setting. The performance of HWNet baseline architecture using just the IAM training data is reported at 0.6336. The use of residual layers gives a significant boost in performance by around 8% which emphasize the generic nature of residual blocks for better learning while increasing the depth of CNN networks. The next big improvement comes when we use variable length representation for word images under multiple scales for better coverage of scale space variation of characters written by different individuals. This is enabled by using either ROI pooling or TPP before the fully connected layers. Here we observe that TPP performs better than ROI since it is a generalization of ROI in multiple scales captured in a pyramidal fashion. In our case, we essentially bring the temporal factor into account by dividing word image along the horizontal direction

Table 3: The list of handwritten datasets used in this work. Here GW, Botany, and Konzilsprotokolle datasets are historical documents written primarily by a single author along with a few assistants(*).

Dataset	Historical	#Words	#Writers
IAM	No	1,15,320	657
GW	Yes	4,894	1*
Botany	Yes	20,004	1*
Konzilsprotokolle (Konz.)	Yes	12,993	1*

Table 4: Ablation studies showing the effect of each of the enhancements to the baseline HWNet architecture on IAM dataset.

HWNet Enhancements	mAP
HWNet	0.6336
HWNet+ResNet (R)	0.7198
HWNet+R+Multi-Scale-ROI (ROI)	0.8457
HWNet+R+Multi-Scale-TPP (TPP)	0.8803
HWNet+R+TPP+Data Augmentation (D)	0.8996
HWNet+R+TPP+D+IIIT-HWS (S)	0.9164
HWNet+R+TPP+D+S+Test-Aug. (HWNet v2)	0.9241

in each pyramid level. We now present the role of different augmentation techniques. Here we observe that using elastic and affine distortion gives around 2% improvement, while the next major improvement is obtained by pre-training the network using IIIT-HWS synthetic dataset. Under this setting, the network is first trained using the synthetic dataset of vocabulary 10K and later fine tuned on IAM dataset, following all architectural changes and data augmentation scheme. Finally, we also perform test time augmentation by extracting features at multiple scales. Here we resize word images at different heights (32, 48, 64) and record the maximum values of feature activation among individual scale representation. The final reported performance using HWNet v2 using TPP is 0.9241.

7.4 Word Spotting Evaluation

7.4.1 Architecture Evaluation

In order to validate the efficiency of baseline HWNet [37] and HWNet v2 architectures with other popular CNN architectures used for classification, we investigate the performance of handwritten word spotting using features obtained from two successful models, (i) AlexNet [39], which was trained on natural images from ImageNet LSVRC data, and (ii) scene text recognition model (JSVZNet) trained on a large scale vocabulary of words [32]. We validate the performance of these networks on IAM [47] dataset. Table 5 reports the word spotting performance for each model and compares it with HWNet. Here ‘Orig’ refers to the model trained with its respective original datasets (e.g. AlexNet on ImageNet and JSVZNet on natural scene text) and ‘IAM’ refers to the model fine tuned on IAM dataset. The ‘Orig’ results (AlexNet and JSVZNet) are low, compared to the other methods for word spotting. However, they are still superior to many of the earlier

Table 5: Comparative mAP evaluation of different deep networks with respect to the HWNet and HWNet v2 (TPP) network on IAM dataset.

Arch.	Orig	IAM	IIIT-HWS	IIIT-HWS+IAM
AlexNet	0.2997	0.4468	*	*
JSVZNet	0.3746	0.4822	*	*
HWNet	*	0.6336	0.5784	0.8061
HWNet v2	*	0.8574	0.6387	0.9241

handcrafted [59] features for this task. We also notice that JSVZNet performs better compared to AlexNet since it is trained for scene text words while the later model is tuned for natural scene images. The results after fine tuning (‘IAM’) on IAM dataset improves the existing results by a good margin. In the last two rows, we present the results of HWNet and HWNet v2 architectures. There is a significant improvement in results from HWNet based architectures w.r.t other architectures when trained on IAM dataset. The last two columns of the table presents the results of only using synthetic data (IIIT-HWS) and along with fine tuning on real data (IIIT-HWS+IAM) separately. Here, the reasonable results that we obtain on just using the synthetic data (column 4) suggest the quality of generated synthetic data which captures real world variations. It also brings an interesting thought, whether in future, does such synthetic data rendering techniques limit the dependency on the availability of real data for training such systems. In section 7.5, we present such an experiment.

7.4.2 State of the Art Comparison

Table 6, presents a detailed comparison between the proposed word representation and other recent methods in the task of word spotting in the query-by-example (QBE) setting on various datasets. The first three rows of the table show non-deep learning methods using engineered features. Here DTW based method uses Vinciarelli [81] features. The Fisher Vector (FV) representation [51] is computed from SIFT features, reduced to 64 dimensions using PCA, and then aggregated into the Fisher Vector. Note that both DTW based method and the Fisher representations are not learned in a supervised setting and thus cannot directly be compared to other methods which are supervised. Here we observe that FV performs better on these datasets compared to pixel level features using DTW. The attributes embedding framework described in KCSR [4] gives a significant boost in the performance. It also uses FV based image representation, and projects both image and text into

Table 6: Quantitative evaluation of word spotting on standard handwritten datasets in query-by-example setting. Here, results for DTW and FV are taken from [4], while all other related works are taken from their respective papers.

Method	IAM	GW	Botany	Konz.
DTW	0.1230	0.6063	-	-
FV	0.1566	0.6272	-	-
KCSR [4]	0.5573	0.9304	0.7577	0.7791
HWNNet [37]	0.8061	0.9484	0.8416	0.7913
PHOCNet [74]	0.7251	0.9671	0.8969	0.9605
TPP-PHOCNet [75]	0.8274	0.9778	0.9123	0.9770
TPP-PHOCNet (BPA) [76]	0.8480	0.9790	0.9605	0.9811
TPP-PHOCNet (CPS) [76]	0.8274	0.9796	0.8081	0.9642
PHOCNet (BPA) [76]	0.8550	0.9758	0.9410	0.9708
Triplet-CNN [83]	0.8158	0.9800	0.5495	0.8215
LSDE [24]	-	0.9131	-	-
HWNNet v2 (ROI)	0.9065	0.9601	0.9401	0.9427
HWNNet v2 (TPP)	0.9241	0.9824	0.9526	0.9347

a PHOC word attribute space and further learns a common subspace where the correlation of both modalities is maximum. The improvement in performance emphasizes the importance of supervised learning to capture the multi-writer styles and its variations where annotated data is available.

The next set of methods consider convolutional networks for extracting features optimum for word spotting. Here, we observe HWNNet [37] based features clearly surpasses the previous method KCSR on all datasets. It shows the robustness of learned features using the deep network and the role of synthetic data to bootstrap the training. The next set of methods in this space use the principle of attribute embedding framework using deep CNN networks. Here, PHOCNet [74] and TPP-PHOCNet [75, 76] uses the output space of CNN as PHOC embedding while Triplet-CNN [83] explores with different embeddings such as PHOC, DCTOW and few semantic embeddings. In the table, we report the best performance of Triplet-CNN across different proposed embeddings. More recently, Gomez et al. [24] presented a novel embedding scheme (LSDE) by learning a subspace which respects edit distance or Levenshtein distance between a pair of samples. Although the performance is inferior from other methods, the notion of edit distance is a valid assumption while considering the string data. Finally, we compare the proposed HWNNet v2 architecture on both variants (ROI, TPP) with its predecessor (HWNNet) and other methods. As we notice HWNNet v2 performs

significantly better for IAM and GW datasets where we report mAP above 0.92 and 0.98 respectively while getting comparable performance on other datasets. We would like to stress here that the boost in performance is not just because of the synthetic data, but also the architectural enhancements and the underlying formulation of learning holistic features using word classification which makes HWNNet v2 different from other networks. As presented in the ablation study, in Table 4, one can notice the performance on IAM dataset even without adding synthetic data (IIIT-HWS), is better than other state-of-the-art networks shown in Table 6.

Since the original HWNNet v2 was trained on a large synthetic dataset, we would like to measure the performance of proposed features on out-of-vocabulary (OOV) words. Note that for the proposed method, the vocabulary comprises of a union of words present in the synthetic dataset along with the training corpus of IAM. Here we obtain an in-vocabulary performance of 0.9223 and OOV of 0.9497 which shows the robustness of features on OOV words and also validates the unbiasedness on increasing the vocabulary size. Here, one of the justifications for the increase in OOV performance is that, in general OOV are larger words (in terms of no. of characters) which gives good contextual information to its representation and thereby easier to retrieve.

7.4.3 Segmentation-Free Word Spotting

In this section, we evaluate the performance of HWNNet v2 representation under noisy word bounding boxes and segmentation-free setting. This is in contrast to the previous evaluation where the segmentation of words are given as part of ground truth and are typically tight. In Fig. 9, we present an ablation study by perturbing the ground truth word segmentation of the test dataset within a certain intersection over union (IoU) range. A similar study of inaccurate cropping has also been presented in [25] for word image semantic retrieval task. In our study, we vary the IoU range between (0.5, 1). Note that the perturbed bounding box is cropped from the original word image which could include surrounding words and noise from the page image. While the query word image is kept intact without perturbation. As shown in the figure, we observe the drop in performance marginal on increasing the IoU range for both IAM and GW datasets. Even at an IoU range of 0.5, we obtain a QBE mAP of 0.8034% and 0.9300% for IAM and GW datasets respectively.

We now extend the evaluation to the segmentation-free scenario by computing our representation on word proposals given by an existing framework from litera-

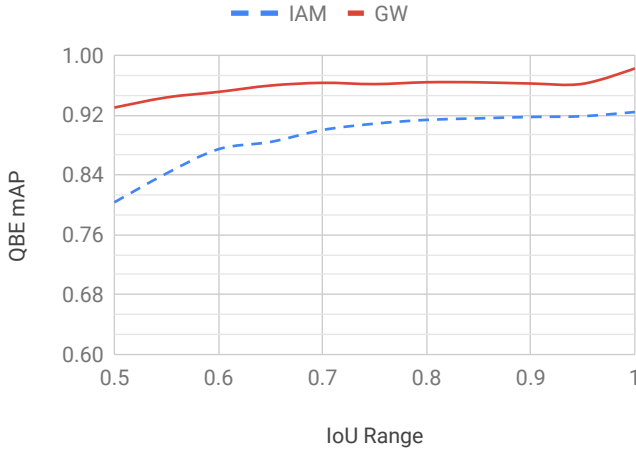


Fig. 9: Ablation study of word spotting in noisy word segmentation. Here we evaluate the word spotting results by perturbing the word segmentations of the test set. The perturbations are done randomly within an IoU range (0.5, 1.0).

ture. Here we use the current state of art method Ctrl-F-Net [84, 85]. More specifically, we use the Ctrl-F-Mini model [85] which has a simplified architecture with better performance. The last row of Table 7, presents the results of HWNet v2 representation as being used as the embedding instead of PHOC. As per the standard evaluation practice, we report the QBE mAP at overlap thresholds of 50% and 25%. Here we observe a significant improvement for IAM dataset of nearly 5%, while for GW dataset we obtain a comparable result. Note that, in contrast to the previous ablation study under noisy segmentation, in the segmentation-free scenario, we obtain a large number of proposals out of which many are false positives. These proposals simply act as distractors in word spotting.

Table 7: QBE mAP evaluation of HWNet v2 representation under segmentation-free scenario. Here we use the word proposals generated using the recent state of art method Ctrl-F-Mini [85]. As per the standard evaluation practice, we report the QBE mAP at overlap thresholds of 50% and 25%.

Embedding	IAM		GW	
	50%	25%	50%	25%
Ctrl-F-Net (DCToW) [84]	0.7200	0.7410	0.9050	0.9700
Ctrl-F-Mini (PHOC) [85]	0.7570	0.7780	0.9160	0.9700
Ctrl-F-Mini (HWNet v2)	0.8200	0.8240	0.9202	0.9665

7.4.4 Query-by-String Spotting Results

In order to show the generic nature of the proposed architecture and its extension for query-by-string (QBS) spotting, in our set of parallel works [35, 36], we have used HWNet architecture for both embedding into word attribute space defined by PHOC [35] and also proposed an end2end architecture [36] which learns a common subspace between a text and image modality. It enables both QBE and QBS based word spotting along with word recognition using a fixed lexicon. Although the description of these works lies beyond the scope of current work, we would like to report the QBS performance reported by these architectures. Here we first report the performance of HWNet (both baseline and v2) features, embedded on to PHOC attributes space. Using the baseline HWNet architecture we obtain a QBS mAP of 0.9158 [35] on IAM dataset, while using the HWNet v2 architecture, we further improve this to 0.9404 [36]. Notice that, the embedding of HWNet onto PHOC attribute space was a two-stage approach. In [36], we propose an end2end scheme using HWNet v2 architecture which directly embeds both image and text into a common subspace. Here we obtain a comparable mAP of 0.9351 on IAM dataset. Please note the reported results are still competitive among the best QBS results shown in TPP-PHOCNet (CPS) [76] which reports an mAP of 0.9342 on IAM dataset.

7.5 Transfer Learning

To better understand the transferability of features from the synthetic domain to the real domain while performing fine-tuning, we employ a similar study as presented in [88]. Fig. 10 compares the performance while doing transfer learning at different layers while keeping the layers before it either freezed or updating them. In the present analysis, we restricted the layers to four ResNet blocks and two fully connected layers immediately after it. We also analyze in three different scenarios: (i) Synth2HW, here the base network is trained on synthetic data (IIIT-HWS), and later fine-tuned on real world handwritten data IAM, (ii) HW2Synth, here the base network is trained on IAM and later fine-tuned on IIIT-HWS and (iii) FineTune where all the layer weights are allowed to update while re-training. Note that, in the first two settings the weights before the particular ResNet block/FC layer is kept freezed. We also report the base network performance while training on Synth and IAM datasets. The performance of Base Synth network is quite less, which indicates the presence of domain gap while Base HW performs fairly good with the enhancements done

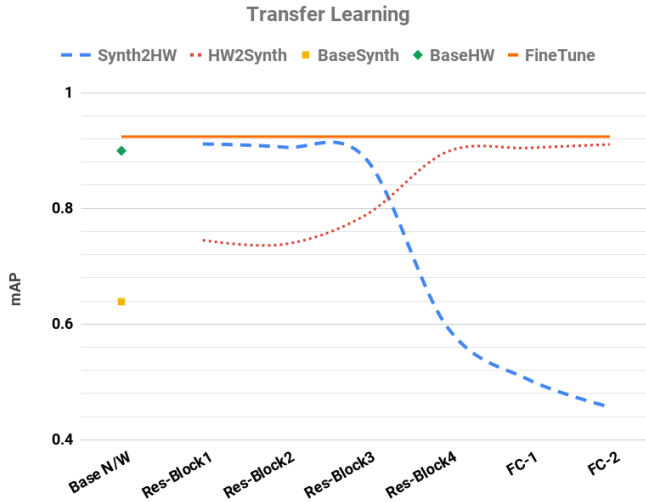


Fig. 10: Graph analyzing the layer for efficient transfer learning.

as part of HWNet v2. Under the three settings of transfer learning, we notice that the best performance is obtained in the third setting of fine tuning where all the weights are simultaneously updated without freezing any layers. Except for the setting of Synth2HW where we keep block 1 frozen, in all other scenarios we obtain inferior results which suggest that initial layer filters learned by the synthetic data are reasonably robust and generalize well to real scenarios.

In Table 8 we present an interesting outcome of transfer learning from synthetic data. Here we experiment the reduced need for real data for training HWNet v2 architecture by varying the amount of training data as compared to previous experiments. Here also we take IAM dataset as our test bench and use a different proportion of real data and compare the performance with architecture which uses full training data. Here full is depicted as 1.0 while 0.0 depicts the use of only synthetic data. Note that all these experiments are first trained on entire synthetic data and later fine-tuned using varying proportions. As one can notice the drop in performance with reduced real training data starts very slowly and surprisingly even using a mere 10% of

Table 8: Evaluation of word spotting using mAP on IAM test dataset by training HWNet v2 with entire synthetic dataset while fine tuning on varying percentage of IAM training data. Here Train=0.0% refers only using synthetic data for training.

Train %	1.0	0.8	0.6	0.4	0.2	0.1	0.0
HWNNet v2	0.9241	0.9150	0.9084	0.9025	0.8773	0.8625	0.6387

real data only drops the performance by 6%. Although this suggests the lesser dependency on real data, we believe this needs a thorough study (out of the scope of current work) to evaluate the differences in domain gap between synthetic data and the target handwritten styles.

7.6 t-SNE Embedding

To better understand the learned representation space, in Fig. 11 we present the t-SNE [42] embedding of word image representation for visualization of higher dimensional feature space. We took the validation set from IAM dataset for t-SNE embedding. The visualization shown here brings interesting insights where we see that the stopwords which occur higher in number are shifted to the periphery of the space where they neatly group into tight clusters. The rest of the significant words from the vocabulary are scattered inside the region. On a closer look, we observe the neighboring sample points belong to the same word or words which are lexically near in space. Please note in the inner region, it is difficult to make out tight clusters since the frequency of these words is quite low. Few of such points are presented along with the actual validation word image taken from the dataset. One can notice the invariance in representation space which clearly take lexical content into account. We also observe smoothness in the representation space where words such as (might, night) and (see, seen) are found closer in the embedding.

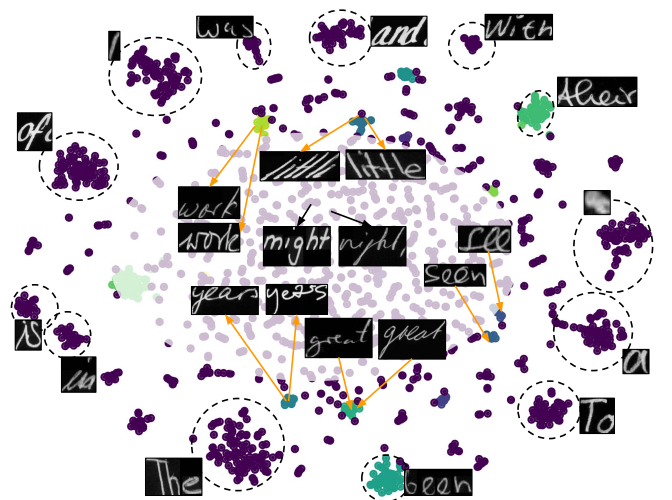


Fig. 11: t-SNE embedding of word image representation taken from the validation set from IAM dataset.

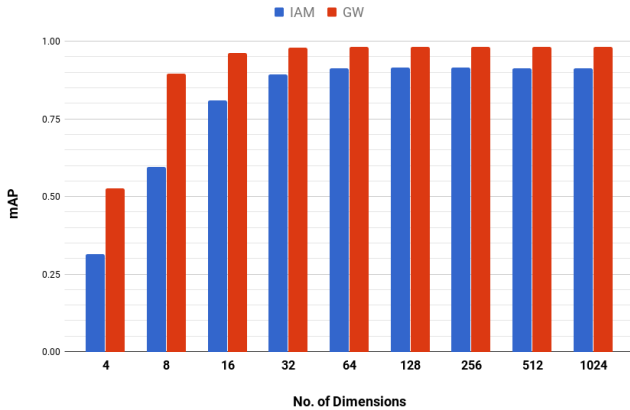


Fig. 12: Evaluation of compression of learned representation using PCA on IAM and GW datasets.

7.7 Compression of Representation

Taking inspirations from our previous analysis on embedding the representation onto a two dimensional space where we gained interesting insights on the similarity of neighbors even in extreme form of compression. We now formally extract a lower dimensional representation of HWNet features using principal component analysis (PCA), which is a popular linear dimensionality reduction technique. We use the validation data to extract the top eigen vectors in the representation space and project each of the test data using them. Fig. 12 shows the performance variation across different compression levels starting from 4 to 1024 on both IAM and GW datasets. Note that original HWNet features are of size 2048. It is interesting to see that there is minimal or no drop in performance in the range of dimensions 32-1024 and we even get a minor improvement in performance for 128 dimensions. This clearly states that the original HWNet network is able to capture non-linear relationships in the data and the final representation space only contains linear components. We obtain an mAP of 0.8942 on IAM using 32 dimensions which is still the state-of-the-art as compared to other related methods reported in Table 6. Note that the performance obtained using mere 8 dimensions (0.5942) is still better than some of the non-deep learning methods.

7.8 Qualitative Results and Failure Scenarios

Fig. 13 shows sample qualitative results obtained under different datasets in the query by example setting using HWNet v2 features. One can notice the robustness of features which make it invariant across different writer variations in IAM, word capitalization forms, and com-

Table 9: The list of printed datasets used in this work. Here both Hindi and Telugu datasets are taken from Digital Library of India [5] corpus.

Dataset	#Pages	#Words
English-1601	310	1,13,008
DLI Hindi (HS1)	1,533	4,20,100
DLI Telugu (TS1)	1,005	1,61,265

mon degradations, as seen in the historical datasets such as Botany and Konzilsprotokolle etc. Fig. 14 presents some of the failure cases where our representation fails to match lexically correct neighbors. Here we show the query image and the top nearest neighbors in the representation space which is incorrect. We also show a sample true positive word image which was lying farther in the representation space. Here top two rows show an inherent ambiguity which was created due to the complexity of handwriting where word “saw” and “love” are being retrieved as “now” and “dove”. In the case of the third row, we observe that stylization of the character ‘L’ created a large impact. In summary, we find the ambiguity/complexity of writing and fine grained similarity in different words to be the major causes of failures.

7.9 Applicability for Printed Documents

In order to validate the performance of the proposed architecture on a different modality such as printed documents, we tested our architecture on a standard book from English and few challenging books taken from DLI corpus [5] in Hindi and Telugu.

English-1601 [86]: This is a book in English titled “Adventures of Sherlock Holmes” written by Arthur Conan Doyle. This was first used in [86] for comparing OCR based results with image search.

DLI Hindi and Telugu [38]: These two datasets, belonging to Hindi and Telugu languages from Indic scripts are part of Digital Library of India (DLI) [5] project. DLI has emerged as one of the largest collections of document images in Indian scripts. Many of the pages present in DLI contains serious forms of document degradation which restricts present day OCR’s and text spotting systems to work efficiently. We take one such subset [38] which was annotated at the level of lines and words and referred to as HS1 and TS1 datasets.

We present the results in Table 10 where we compare HWNet v2 (TPP) with previous methods. Note that the previous methods, Yalniz et al. [86] and



Fig. 13: Qualitative results of word spotting. In each row, the leftmost image is the query and remaining are the top retrieved word images based on features similarity. Here (a-d) refers to images taken from IAM, GW, Botany and Konzilsprotokolle datasets respectively. The last two rows (e-f) shows results from printed dataset containing degraded Hindi and Telugu books of the DLI corpus respectively.

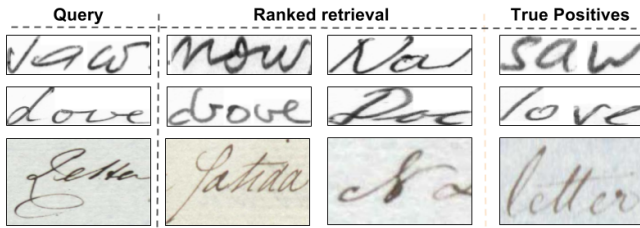


Fig. 14: Sample failure case images where the representation fails to match lexically correct neighbors.

Krishnan et al. [38] use features from BOW pipeline which is essentially unsupervised in nature and not directly comparable with neural codes which are supervised. We would like to contrast the advantages of supervised learning and also baseline the performance on these datasets with deep features. Here for English dataset, we just use the pre-trained model from IIT-HWS without any fine-tuning, while for Hindi and Telugu datasets, we perform fine-tuning

on the training corpus of these datasets respectively. From the results, we notice that the performance of word spotting has improved significantly on all these datasets and for printed English, one could directly use HWNet v2 as off-the-shelf for various document tasks. The improvement of results in Hindi and Telugu also suggests that such an architecture can be used for various languages with wide variations in scripts and language constructs. One can also notice the amount of degradation in the retrieved words from the qualitative

Table 10: Quantitative evaluation of word spotting on printed datasets.

Method	Supervision	English	Hindi	Telugu
Yalniz et.al [86]	No	0.9300	-	-
Krishnan et.al [38]	No	-	0.6055	0.7438
HWNNet v2 (TPP)	Yes	0.9570	0.9509	0.9582

results shown in the last two rows of Fig. 13 which indicates the robustness of the proposed features.

7.10 Implementation Details

HWNet v2 network is trained using stochastic gradient descent algorithm with momentum. We set the momentum factor to be 0.9 and the learning rate is set as $1e-2$ while training from scratch on synthetic data. In the case of fine tuning, the learning rate is initialized from $1e-3$ and manually reduced by a factor of 10 once the loss does not change within a certain threshold in last five epochs. The weights are initialized using He initialization [28]. With respect to data augmentation, we perform on the fly augmentation with 50% probability whether to augment the current sample from the mini-batch. For elastic distortion, we set the hyper-parameters $\alpha = 0.8, \sigma = 0.08$ denoted as scaling and smoothing parameters [71], which regulates the amount of distortion to apply. For affine transformation, we randomly pick whether to rotate, shear or pad. The rotation and shear angles are sampled in the range of $(-5, 15)$ and $(-0.5, 0.5)$ degrees respectively. For bringing translation in-variance, we randomly insert padding in the four boundaries within a range of 0-20 pixels. In our experiments for the segmentation-free scenario, while training the models we also perturbed the ground truth bounding boxes of training word images within an IoU range of $(0.75, 1.0)$ to learn features robust against the noise while testing.

We use NVIDIA GeForce GTX 1080 Ti GPUs for all our experimentation and the codes are written using PyTorch 0.2 library. On a batch size of 8, our code takes GPU RAM of around 6.5GB and 1.4GB for training and inference respectively. The model roughly takes around 10 milliseconds for computing representation for each word image.

7.11 Release of Datasets and Codes

For the reproducibility of research and use of HWNet v2 features for different document processing tasks, we have released the IIIT-HWS synthetic dataset, pre-trained network files of HWNet v2 architecture along with codes for extracting features for word images. More details are shared in the project page².

² <http://cvit.iiit.ac.in/research/projects/cvit-projects/hwnet>

8 Conclusion and Future Work

We introduce a generic deep convolutional framework for learning word image representation for document images. The underlying architecture HWNet v2 uses synthetic data for efficient pre-training and also uses various data augmentation schemes which mimic the natural process of text creation in documents. We further provide different insights into the fine tuning process and also understand the invariances learned at various layers using some recent visualization techniques. We successfully demonstrate the robustness of learned representation in terms of both performance and dimensionality of final representation, on challenging historical manuscripts in both handwritten and printed modalities.

As part of future work, we would like to explore the granularity of representation at the level of patches by augmenting the final representation with intermediate layer activations. We believe such an enriched representation would capture local information which would be useful to distinguish between classes with minimum edit distance. We are also exploring the use of attribute [4] information as conditional data while learning the final representation. In this direction, our initial results which has been accepted in [36] looks promising for word spotting.

References

1. Aldavert, D., Rusinol, M., Toledo, R., Lladós, J.: Integrating visual and textual cues for query-by-string word spotting. In: ICDAR (2013) 3, 4
2. Aldavert, D., Rusinol, M., Toledo, R., Lladós, J.: A study of bag-of-visual-words representations for handwritten keyword spotting. IJDAR (2015) 2, 3, 4
3. Almazán, J., Gordo, A., Fornés, A., Valveny, E.: Segmentation-free word spotting with exemplar SVMs. PR (2014) 3, 4, 5
4. Almazán, J., Gordo, A., Fornés, A., Valveny, E.: Word spotting and recognition with embedded attributes. PAMI (2014) 1, 2, 3, 4, 11, 12, 13, 18
5. Ambati, V., N.Balakrishnan, Reddy, R., Pratha, L., Jawahar, C.V.: The Digital Library of India Project: Process, Policies and Architecture. In: ICDL (2007) 16
6. Axler, G., Wolf, L.: Toward a dataset-agnostic word segmentation method. In: ICIP (2018) 5
7. Balasubramanian, A., Meshesha, M., V.Jawahar, C.: Retrieval from document image collections. In: DAS (2006) 3
8. Bengio, Y., Louradour, J., Collobert, R., Weston, J.: Curriculum learning. In: ICML (2009) 9
9. Causer, T., Wallace, V.: Building a volunteer community: results and findings from transcribe bentham. Digital Humanities Quarterly (2012) 6
10. Chen, K., Seuret, M., Liwicki, M., Hennebert, J., Ingold, R.: Page segmentation of historical document images with convolutional autoencoders. In: ICDAR (2015) 2

11. Csurka, G., Dance, C., Fan, L., Willamowski, J., Bray, C.: Visual categorization with bags of keypoints. In: Workshop on statistical learning in computer vision, ECCV (2004) [2](#), [4](#)
12. Dalal, N., Triggs, B.: Histograms of oriented gradients for human detection. In: CVPR (2005) [2](#), [4](#)
13. Deerwester, S., Dumais, S.T., Furnas, G.W., Landauer, T.K., Harshman, R.: Indexing by latent semantic analysis. *Journal of the American society for information science* (1990) [4](#)
14. Deng, J., Dong, W., Socher, R., Li, L.J., Li, K., Fei-Fei, L.: ImageNet: A Large-Scale Hierarchical Image Database. In: CVPR09 (2009) [2](#), [5](#)
15. Donahue, J., Jia, Y., Vinyals, O., Hoffman, J., Zhang, N., Tzeng, E., Darrell, T.: Decaf: A deep convolutional activation feature for generic visual recognition. In: ICML (2014) [9](#)
16. Everingham, M., Van Gool, L., Williams, C.K.I., Winn, J., Zisserman, A.: The pascal visual object classes (VOC) challenge. *IJCV* (2010) [5](#)
17. Fischer, A., Frinken, V., Bunke, H., Suen, C.Y.: Improving HMM-based keyword spotting with character language models. In: 2013 12th International Conference on Document Analysis and Recognition (2013) [1](#)
18. Fischer, A., Keller, A., Frinken, V., Bunke, H.: Lexicon-free handwritten word spotting using character HMMs. *PRL* (2012) [6](#)
19. Ghosh, S., Valveny, E.: Text box proposals for handwritten word spotting from documents. *IJDAR* (2018) [5](#)
20. Ghosh, S.K., Valveny, E.: A sliding window framework for word spotting based on word attributes. In: *IbPRIA* (2015) [5](#)
21. Giotis, A.P., Sfikas, G., Gatos, B., Nikou, C.: A survey of document image word spotting techniques. *Pattern Recogn.* (2017) [3](#)
22. Girshick, R.: Fast r-cnn. In: *ICCV* (2015) [8](#)
23. Girshick, R., Donahue, J., Darrell, T., Malik, J.: Rich feature hierarchies for accurate object detection and semantic segmentation. In: *CVPR* (2014) [10](#)
24. Gómez, L., Rusinol, M., Karatzas, D.: LSDE: Levenshtein space deep embedding for query-by-string word spotting. In: *ICDAR* (2017) [3](#), [13](#)
25. Gordo, A., Almazán, J., Murray, N., Perronin, F.: LEWIS: latent embeddings for word images and their semantics. In: *ICCV* (2015) [13](#)
26. Harley, A.W., Ufkes, A., Derpanis, K.G.: Evaluation of deep convolutional nets for document image classification and retrieval. In: *ICDAR* (2015) [2](#)
27. Harris, C., Stephens, M.: A combined corner and edge detector. In: *Alvey vision conference* (1988) [4](#)
28. He, K., Zhang, X., Ren, S., Sun, J.: Delving deep into rectifiers: Surpassing human-level performance on imagenet classification. In: *ICCV* (2015) [18](#)
29. He, K., Zhang, X., Ren, S., Sun, J.: Deep residual learning for image recognition. In: *CVPR* (2016) [8](#)
30. Ioffe, S., Szegedy, C.: Batch normalization: Accelerating deep network training by reducing internal covariate shift. *CoRR* (2015) [8](#)
31. Jaderberg, M., Simonyan, K., Vedaldi, A., Zisserman, A.: Reading text in the wild with convolutional neural networks. *IJCV* (2014) [4](#)
32. Jaderberg, M., Simonyan, K., Vedaldi, A., Zisserman, A.: Synthetic data and artificial neural networks for natural scene text recognition. *CoRR* (2014) [4](#), [6](#), [12](#)
33. Jaderberg, M., Vedaldi, A., Zisserman, A.: Deep features for text spotting. In: *ECCV* (2014) [4](#)
34. Kovalchuk, A., Wolf, L., Dershowitz, N.: A simple and fast word spotting method. In: *ICFHR* (2014) [5](#)
35. Krishnan, P., Dutta, K., Jawahar, C.V.: Deep feature embedding for accurate recognition and retrieval of handwritten text. In: *ICFHR* (2016) [3](#), [5](#), [14](#)
36. Krishnan, P., Dutta, K., Jawahar, C.V.: Word spotting and recognition using deep embedding. In: *DAS* (2018) [5](#), [14](#), [18](#)
37. Krishnan, P., Jawahar, C.V.: Matching handwritten document images. In: *ECCV* (2016) [2](#), [3](#), [5](#), [7](#), [12](#), [13](#)
38. Krishnan, P., Shekhar, R., Jawahar, C.: Content level access to digital library of india pages. In: *ICVGIP* (2012) [16](#), [17](#)
39. Krizhevsky, A., Sutskever, I., Hinton, G.E.: Imagenet classification with deep convolutional neural networks. In: *NIPS* (2012) [2](#), [4](#), [6](#), [7](#), [9](#), [12](#)
40. Kumar, A., Jawahar, C.V., Manmatha, R.: Efficient Search in Document Image Collections. In: *ACCV* (2007) [3](#)
41. Lowe, D.G.: Distinctive image features from scale-invariant keypoints. *IJCV* (2004) [2](#), [4](#)
42. Maaten, L.v.d., Hinton, G.: Visualizing data using t-SNE. *JMLR* (2008) [15](#)
43. Mahendran, A., Vedaldi, A.: Understanding deep image representations by inverting them. In: *CVPR* (2015) [10](#)
44. Malisiewicz, T., Gupta, A., Efros, A.A.: Ensemble of exemplar-SVMs for object detection and beyond. In: *ICCV* (2011) [4](#)
45. Manmatha, R., Han, C., Riseman, E.M.: Word spotting: A new approach to indexing handwriting. In: *CVPR* (1996) [1](#), [2](#), [3](#), [6](#)
46. Marti, U., Bunke, H.: Using a statistical language model to improve the performance of an HMM-based cursive handwriting recognition system. *IJPRAI* (2001) [2](#), [3](#)
47. Marti, U., Bunke, H.: The IAM-database: an English sentence database for offline handwriting recognition. *IJDAR* (2002) [3](#), [6](#), [11](#), [12](#)
48. Meshesha, M., Jawahar, C.V.: Matching Word Images for Content-based Retrieval from Printed Document Images. *IJDAR* (2008) [3](#)
49. Myers, C., Rabiner, L., Rosenberg, A.: Performance tradeoffs in dynamic time warping algorithms for isolated word recognition. *Acoustics, Speech and Signal Processing, IEEE Transactions on* (1980) [3](#)
50. Perronnin, F., Dance, C.: Fisher kernels on visual vocabularies for image categorization. In: *CVPR* (2007) [2](#)
51. Perronnin, F., Rodríguez-Serrano, J.A.: Fisher kernels for handwritten word-spotting. In: *ICDAR* (2009) [4](#), [12](#)
52. Poznanski, A., Wolf, L.: CNN-N-Gram for handwriting word recognition. In: *CVPR* (2016) [2](#), [5](#)
53. Pratikakis, I., Zagoris, K., Gatos, B., Puigcerver, J., Toselli, A.H., Vidal, E.: Icfhr2016 handwritten keyword spotting competition (h-kws 2016). In: *ICFHR* (2016) [11](#)
54. Rath, T.M., Manmatha, R.: Word image matching using dynamic time warping. In: *CVPR* (2003) [2](#), [3](#)
55. Rath, T.M., Manmatha, R.: Word spotting for historical documents. *IJDAR* (2007) [11](#)
56. Razavian, A.S., Azizpour, H., Sullivan, J., Carlsson, S.: CNN features off-the-shelf: An astounding baseline for recognition. In: *CVPR* (2014) [2](#), [9](#)
57. Ren, S., He, K., Girshick, R., Sun, J.: Faster R-CNN: Towards real-time object detection with region proposal networks. In: *Advances in neural information processing systems* (2015) [5](#)
58. Rodriguez, J.A., Perronnin, F.: Local gradient histogram features for word spotting in unconstrained handwritten documents. In: *ICFHR* (2008) [2](#), [3](#), [4](#)

59. Rodríguez-Serrano, J.A., Perronnin, F.: A model-based sequence similarity with application to handwritten word spotting. *PAMI* (2012) [12](#)
60. Rohlicek, J.R., Russell, W., Roukos, S., Gish, H.: Continuous hidden markov modeling for speaker-independent word spotting. In: *ICASSP* (1989) [3](#)
61. Ros, G., Sellart, L., Materzynska, J., Vazquez, D., Lopez, A.M.: The synthia dataset: A large collection of synthetic images for semantic segmentation of urban scenes. In: *CVPR* (2016) [6](#)
62. Rosten, E., Drummond, T.: Machine learning for high-speed corner detection. *ECCV* (2006) [4](#)
63. Rothacker, L., Rusinol, M., Fink, G.A.: Bag-of-features HMMs for segmentation-free word spotting in handwritten documents. In: *ICDAR* (2013) [3](#), [5](#)
64. Rothacker, L., Sudholt, S., Rusakov, E., Kasperidus, M., Fink, G.A.: Word hypotheses for segmentation-free word spotting in historic document images. In: *ICDAR* (2017) [5](#)
65. Roy, P.P., Rayar, F., Ramel, J.Y.: Word spotting in historical documents using primitive codebook and dynamic programming. *Image Vision Comput.* (2015) [2](#)
66. Rozantsev, A., Lepetit, V., Fua, P.: On rendering synthetic images for training an object detector. *CVIU* (2015) [6](#)
67. Rusiñol, M., Aldavert, D., Toledo, R., Lladós, J.: Browsing heterogeneous document collections by a segmentation-free word spotting method. In: *ICDAR* (2011) [1](#), [3](#), [4](#), [5](#)
68. Rusiñol, M., Aldavert, D., Toledo, R., Lladós, J.: Efficient segmentation-free keyword spotting in historical document collections. *PR* (2015) [2](#), [4](#)
69. Sakoe, H., Chiba, S.: Dynamic programming algorithm optimization for spoken word recognition. *Acoustics, Speech and Signal Processing, IEEE Transactions on* (1978) [3](#)
70. Shekhar, R., Jawahar, C.V.: Word image retrieval using bag of visual words. In: *DAS* (2012) [3](#), [4](#), [9](#)
71. Simard, P.Y., Steinkraus, D., Platt, J.C.: Best practices for convolutional neural networks applied to visual document analysis. In: *ICDAR* (2003) [9](#), [18](#)
72. Simonyan, K., Zisserman, A.: Very deep convolutional networks for large-scale image recognition. *CoRR* (2014) [4](#), [5](#), [6](#), [8](#)
73. Sivic, J., Zisserman, A.: Video Google: A text retrieval approach to object matching in videos. In: *ICCV* (2003) [2](#), [4](#)
74. Sudholt, S., Fink, G.A.: PHOCNet: A deep convolutional neural network for word spotting in handwritten documents. In: *ICFHR* (2016) [2](#), [3](#), [5](#), [13](#)
75. Sudholt, S., Fink, G.A.: Evaluating word string embeddings and loss functions for CNN-based word spotting. In: *ICDAR* (2017) [3](#), [5](#), [9](#), [13](#)
76. Sudholt, S., Fink, G.A.: Attribute CNNs for word spotting in handwritten documents. *International Journal on Document Analysis and Recognition (IJ DAR)* (2018) [2](#), [5](#), [13](#), [14](#)
77. Szegedy, C., Liu, W., Jia, Y., Sermanet, P., Reed, S., Anguelov, D., Erhan, D., Vanhoucke, V., Rabinovich, A.: Going deeper with convolutions. In: *CVPR* (2015) [4](#), [6](#), [8](#)
78. Szegedy, C., Zaremba, W., Sutskever, I., Bruna, J., Erhan, D., Goodfellow, I., Fergus, R.: Intriguing properties of neural networks. *arXiv preprint arXiv:1312.6199* (2013) [10](#)
79. Terasawa, K., Tanaka, Y.: Slit style HOG feature for document image word spotting. In: *ICDAR* (2009) [2](#), [3](#), [4](#)
80. Toselli, A.H., Vidal, E., Romero, V., Frinken, V.: HMM word graph based keyword spotting in handwritten document images. *Information Sciences* (2016) [1](#)
81. Vinciarelli, A., Bengio, S.: Offline cursive word recognition using continuous density hidden markov models trained with PCA or ICA features. In: *ICPR* (2002) [12](#)
82. Wang, J., Yang, J., Yu, K., Lv, F., Huang, T., Gong, Y.: Locality-constrained linear coding for image classification. In: *CVPR* (2010) [2](#)
83. Wilkinson, T., Brun, A.: Semantic and verbatim word spotting using deep neural networks. In: *ICFHR* (2016) [2](#), [3](#), [5](#), [13](#)
84. Wilkinson, T., Lindstrom, J., Brun, A.: Neural Ctrl-F: segmentation-free query-by-string word spotting in handwritten manuscript collections. In: *ICCV* (2017) [5](#), [14](#)
85. Wilkinson, T., Lindström, J., Brun, A.: Neural word search in historical manuscript collections. *CoRR abs/1812.02771* (2018) [5](#), [14](#)
86. Yalniz, I.Z., Manmatha, R.: An efficient framework for searching text in noisy document images. In: *DAS* (2012) [3](#), [4](#), [16](#), [17](#)
87. Yang, J., Yu, K., Gong, Y., Huang, T.: Linear spatial pyramid matching using sparse coding for image classification. In: *CVPR* (2009) [2](#)
88. Yosinski, J., Clune, J., Bengio, Y., Lipson, H.: How transferable are features in deep neural networks? In: *NIPS* (2014) [9](#), [14](#)
89. Yosinski, J., Clune, J., Nguyen, A., Fuchs, T., Lipson, H.: Understanding neural networks through deep visualization. *arXiv preprint arXiv:1506.06579* (2015) [10](#)
90. Zeiler, M.D., Fergus, R.: Visualizing and understanding convolutional networks. In: *ECCV* (2014) [10](#)